J. Phys.: Condens. Matter **20** (2008) 315011 (11pp) doi:10.1088/0953-8984/20/31/315011

Theory of the leak-rate of seals

B N J Persson and C Yang

Institut für Festkörperforschung, Forschungszentrum Jülich, D-52425 Jülich, Germany

Received 18 April 2008, in final form 4 June 2008
Published 17 July 2008
Online at stacks.iop.org/JPhysCM/20/315011

Abstract

Seals are extremely useful devices to prevent fluid leakage. However, the exact mechanism of roughness induced leakage is not well understood. We present a theory of the leak-rate of seals, which is based on percolation theory and a recently developed contact mechanics theory. We study both static and dynamic seals. We present molecular dynamics results which show that when two elastic solids with randomly rough surfaces are squeezed together, as a function of increasing magnification or decreasing squeezing pressure, a non-contact channel will percolate when the (relative) projected contact area, A/A_0, is of the order 0.4, in accordance with percolation theory. We suggest a simple experiment which can be used to test the theory.

(Some figures in this article are in colour only in the electronic version)

1. Introduction

A seal is a device for closing a gap or making a joint fluid tight [1]. Seals play a crucial role in many modern engineering devices, and the failure of seals may result in catastrophic events, such as the Challenger disaster. In spite of its apparent simplicity, it is still not possible to theoretically predict the leak-rate and (for dynamic seals) the friction forces [2] for seals. The main problem is the influence of surface roughness on the contact mechanics at the seal–substrate interface. Most surfaces of engineering interest have surface roughness on a wide range of length scales [3], e.g, from cm to nm, which will influence the leak-rate and friction of seals, and accounting for the whole range of surface roughness is impossible using standard numerical methods, such as the finite element method.

In this paper we will analyze the role of surface roughness on seals. We will use a recently developed contact mechanics theory [4–9] to calculate the leak-rate of static seals. We assume that purely elastic deformation occurs in the solids, which is the case for rubber seals. For metal seals, strong plastic deformation often occurs in the contact region.

The theory developed below is based on studying the interface between the rubber and the hard countersurface (usually a metal) at different magnifications ζ. At low magnification the surfaces appear flat and the contact between them appears to be complete (i.e., no leak channels can be observed). However, when we increase the magnification we observe surface roughness at the interface, and, in general, non-contact regions. As the magnification increases, we will observe more and more (short-wavelength) roughness, and the (apparent) contact area $A(\zeta)$ between the solids will decrease. At high enough magnification, for $\zeta = \zeta_c$, a non-contact (percolation) channel will appear, through which fluid will flow, from the high pressure side (pressure P_a) to the low pressure side (pressure P_b), see figure 1. We denote the most narrow passage between the two surfaces along the percolation path as the critical constriction. When the magnification increases further more percolation channels will be observed, but these channels will have more narrow constrictions than those for the first channel which appears at the percolation threshold ($\zeta = \zeta_c$).

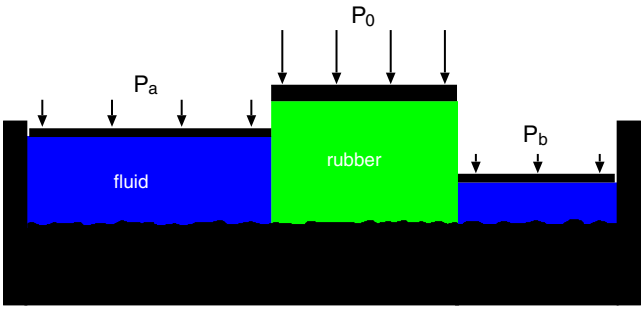

Figure 1. Rubber seal (schematic). The liquid on the left-hand side is under the hydrostatic pressure P_a and the liquid to the right under the pressure P_b (usually, P_b is the atmospheric pressure). The pressure difference $\Delta P = P_a - P_b$ results in liquid flow at the interface between the rubber seal and the rough substrate surface. The volume of liquid flow per unit time is denoted by $\dot{Q}$, and depends on the squeezing pressure P_0 acting on the rubber seal.

The picture described above for the leakage of seals has already been presented by one of the present authors [3, 10]. However, recent developments in contact mechanics now allow us to present a more accurate analysis of the leakage

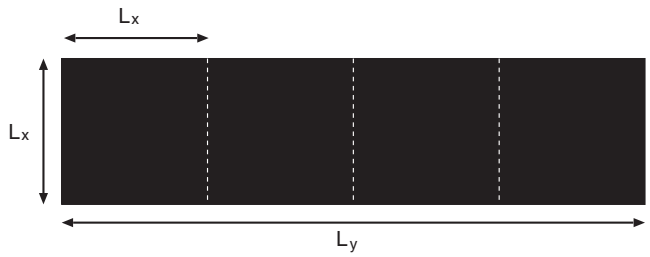

Figure 2. The rubber–countersurface apparent contact area is rectangular $L_x \times L_y$. We 'divide' it into $N = L_y/L_x$ square areas with side $L = L_x$ and area $A_0 = L^2$.

process. In this paper we extend the theory of [10] and present numerical results for the size of the critical constriction and for the leak-rate.

In section 2 we describe the basic picture used to calculate the leak-rate of static seals. The theory is based on a recently developed contact mechanics model [5–9] that accurately takes into account the elastic coupling between the contact regions in the nominal rubber–substrate contact area. Earlier contact mechanics models, such as the Greenwood–Williamson [11] model or the model of Bush *et al* [12], neglect this elastic coupling which results in highly incorrect relations between the squeezing pressure and the interfacial separation. In section 3 we present numerical results for the size of the critical constriction and for the leak-rate. In section 4 we present molecular dynamics results which illustrate how the contact between the two solids changes as the magnification ζ increases. We find that the percolation channel is formed when $\zeta = \zeta_c$, where $A(\zeta_c)/A_0 \approx 0.4$, in accordance with percolation theory [13]. In section 5 we improve the theoretical picture of how to understand static seals. In section 6 we compare the theory with experimental data. In section 7 we present some comments related to the non-uniform seal pressure distribution, the role of adhesion and rubber viscoelasticity. In section 8 we study dynamical (linear reciprocal motion) seals at low sliding velocities. In section 9 we suggest a simple experiment to test the theory. Section 10 contains the summary and the conclusion.

2. Theory

We first briefly review the basic picture on which our calculations of the leak-rate are based [10]. Assume that the nominal contact region between the rubber and the hard countersurface is rectangular with area $L_x \times L_y$, see figure 2. We assume a high pressure fluid region for $x < 0$ and a low pressure region for $x > L_x$. We now divide the contact region into squares with side $L_x = L$ and area $A_0 = L^2$ (this assumes that $N = L_y/L_x$ is an integer, but this restriction does not affect the final result). Now, let us study the contact between the two solids within one of the squares as we change the magnification ζ. We define $\zeta = L/\lambda$, where λ is the resolution. We study how the apparent contact area (projected on the xy-plane), $A(\zeta)$, between the two solids depends on the magnification ζ. At the lowest magnification we cannot observe any surface roughness, and the contact between the solids appears to be complete i.e., $A(1) = A_0$. As we increase the magnification we will observe some interfacial roughness, and the (apparent) contact area will decrease, see figures 3 and 4. At high enough magnification, say $\zeta = \zeta_c$, a percolating path of non-contact area will eventually be observed, see figure 4. The most narrow constriction along the percolation path has a lateral size $\lambda_c = L/\zeta_c$ and the surface separation at this point is denoted by $u_c = u_1(\zeta_c)$ and is given

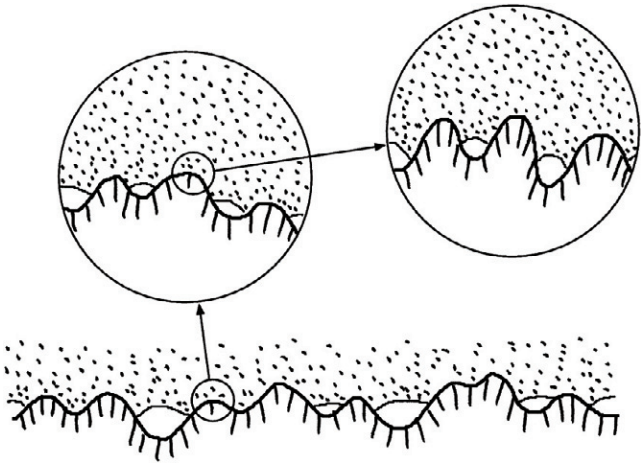

Figure 3. An rubber block (dotted area) in adhesive contact with a hard rough substrate (dashed area). The substrate has roughness on many different length scales and the rubber makes partial contact with the substrate on all length scales. When a contact area is studied at low magnification it appears as if complete contact occurs, but when the magnification is increased it is observed that in reality only partial contact occurs.

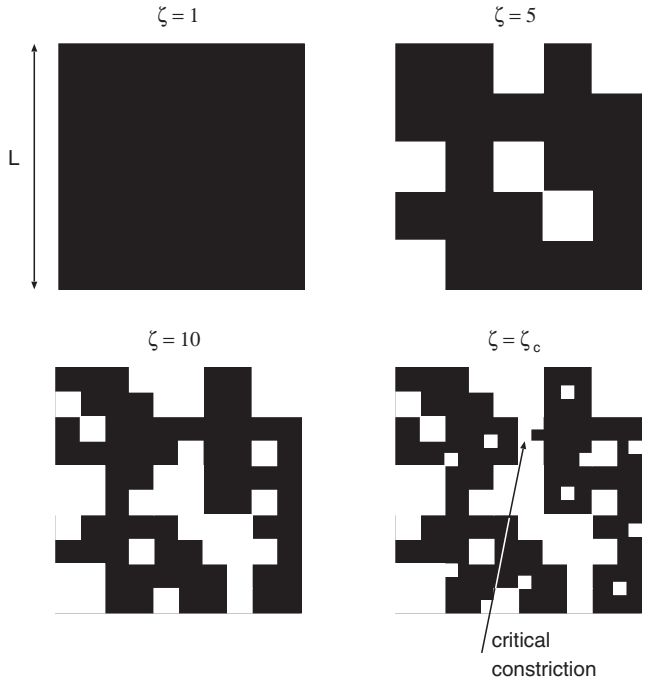

Figure 4. The contact region at different magnifications (schematic). Note that at the point where the non-contact area (white area) percolates $A(\zeta_c) \approx 0.4A_0$, while there appears to be complete contact between the surfaces at the lowest magnification $\zeta = 1$: $A(1) = A_0$.

by a recently developed contact mechanics theory (see below). As we continue to increase the magnification we find more percolating channels between the surfaces, but as these have narrower constrictions than the first channel which appears at $\zeta = \zeta_c$ for the moment we will neglect their contribution to the leak-rate (see also section 5). Thus, in this section we will assume that the leak-rate is determined by the critical constriction.

A first rough estimate of the leak-rate is obtained by assuming that all the leakage occurs through the critical percolation channel, and that the whole pressure drop $\Delta P = P_a - P_b$ (where P_a and P_b is the pressure to the left and right of the seal) occurs over the critical constriction (of width and length $\lambda_c \approx L/\zeta_c$ and height $u_c = u_1(\zeta_c)$). Thus for an incompressible Newtonian fluid, the volume flow per unit time through the critical constriction will be

$$\dot{Q} = M\Delta P, \tag{1}$$

where

$$M = \alpha \frac{u_1^3(\zeta_c)}{12\eta}, \tag{2}$$

where η is the fluid viscosity. In deriving (1) we have assumed laminar flow and that $u_c \ll \lambda_c$, which is always satisfied in practice. We have also assumed a no-slip boundary condition on the solid walls. This assumption is not always satisfied at the micro or nanoscale, but is likely to be a very good approximation in the present case owing to surface roughness which occurs at length scales shorter than the size of the critical constriction. In (2) we have introduced a factor α which depends on the exact shape of the critical constriction, but which is expected to be of order unity. Since there are $N = L_y/L_x$ square areas in the rubber–countersurface (apparent) contact area, we get the total leak-rate

$$\dot{Q} = \frac{L_y}{L_x} M\Delta P. \tag{3}$$

To complete the theory we must calculate the separation $u_c = u_1(\zeta_c)$ of the surfaces at the critical constriction. We first determine the critical magnification ζ_c by assuming that the apparent relative contact area at this point is given by site percolation theory. Thus, the relative contact area $A(\zeta)/A_0 \approx 1 - p_c$, where p_c is the so called site percolation threshold [13]. For infinite-sized systems $p_c \approx 0.696$ for a hexagonal lattice and 0.593 for a square lattice [13]. For finite-sized systems the percolation will, on average, occur for (slightly) smaller values of p, and fluctuations in the percolation threshold will occur between different realization of the same physical system. We will address this problem again later (see section 4) but for now we take $p_c \approx 0.6$ so that $A(\zeta_c)/A_0 \approx 0.4$ will determine the critical magnification $\zeta = \zeta_c$.

The (apparent) relative contact area $A(\zeta)/A_0$ at the magnification ζ can be obtained using the contact mechanics formalism developed elsewhere [4, 6–9], where the system is studied at different magnifications ζ, see figure 3. We have [4, 5]

$$\frac{A(\zeta)}{A_0} = \frac{1}{(\pi G)^{1/2}} \int_0^{P_0} \mathrm{d}\sigma\ \mathrm{e}^{-\sigma^2/4G} = \mathrm{erf}\left(\frac{P_0}{2G^{1/2}}\right)$$

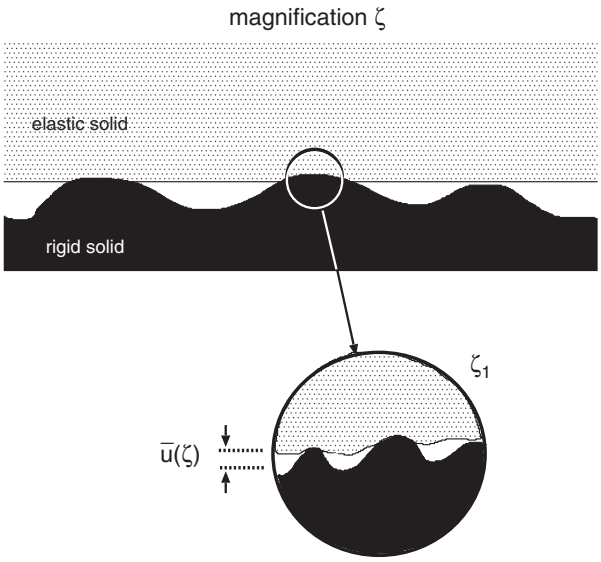

Figure 5. An asperity contact region observed at the magnification ζ. It appears that complete contact occurs in the asperity contact region, but upon increasing the magnification it is observed that the solids are separated by an average distance $\bar{u}(\zeta)$.

where

$$G(\zeta) = \frac{\pi}{4}\left(\frac{E}{1-\nu^2}\right)^2 \int_{q_0}^{\zeta q_0} \mathrm{d}q q^3 C(q)$$

where the surface roughness power spectrum

$$C(q) = \frac{1}{(2\pi)^2} \int \mathrm{d}^2x \langle h(\mathbf{x})h(\mathbf{0})\rangle \mathrm{e}^{-\mathrm{i}\mathbf{q}\cdot\mathbf{x}}$$

where $\langle\cdots\rangle$ stands for ensemble average. Here E and ν are the Young's elastic modulus and the Poisson ratio of the rubber. The height profile $h(\mathbf{x})$ of the rough surface can be measured routinely today on all relevant length scales using optical and stylus experiments.

We define $u_1(\zeta)$ to be the (average) height separating the surfaces which appear to come into contact when the magnification decreases from ζ to $\zeta - \Delta\zeta$, where $\Delta\zeta$ is a small (infinitesimal) change in the magnification. $u_1(\zeta)$ is a monotonically decreasing function of ζ, and can be calculated from the average interfacial separation $\bar{u}(\zeta)$ and $A(\zeta)$ using (see [9])

$$u_1(\zeta) = \bar{u}(\zeta) + \bar{u}'(\zeta)A(\zeta)/A'(\zeta).$$

The quantity $\bar{u}(\zeta)$ is the average separation between the surfaces in the apparent contact regions observed at the magnification ζ, see figure 5. It can be calculated from [9]

$$\bar{u}(\zeta) = \sqrt{\pi} \int_{\zeta q_0}^{q_1} \mathrm{d}q\ q^2 C(q) w(q) \times \int_{p(\zeta)}^{\infty} \mathrm{d}p'\ \frac{1}{p'}\left[\gamma + 3(1-\gamma)P^2(q, p', \zeta)\right] \times \mathrm{e}^{-[w(q,\zeta)p'/E^*]^2},$$

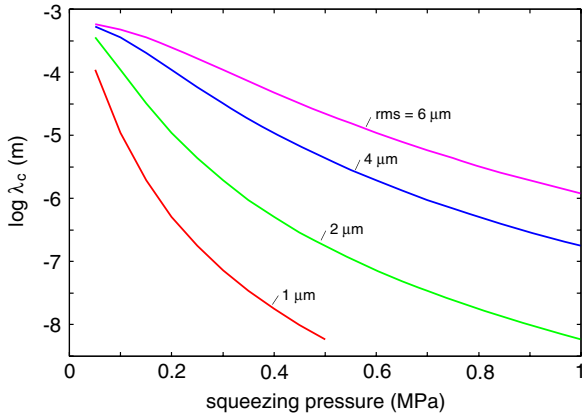

Figure 6. The lateral size $\lambda_c = \lambda(\zeta_c)$ of the critical constriction of the percolation channel, as a function of the applied normal (or squeezing) pressure P_0. Results are shown for self-affine fractal surfaces with the Hurst exponent $H = 0.8$ (or fractal dimension $D_f = 2.2$), and for surfaces with the root-mean-square roughness (rms) 1, 2, 4 and 6 μm.

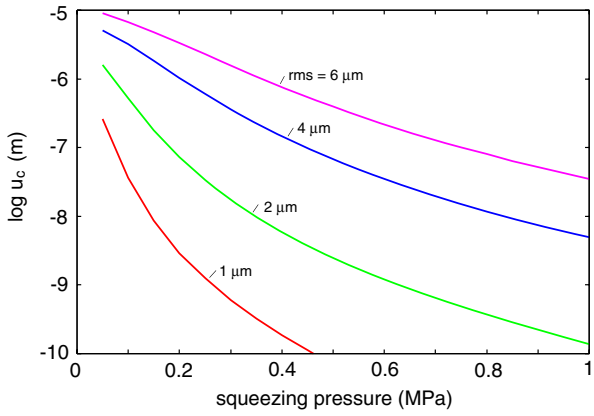

Figure 7. The interfacial separation $u_c = u_1(\zeta_c)$ at the critical constriction of the percolation channel, as a function of the applied normal (or squeezing) pressure P_0. Results are shown for self-affine fractal surfaces with the Hurst exponent $H = 0.8$ (or fractal dimension $D_f = 2.2$), and for surfaces with the root-mean-square roughness (rms) 1, 2, 4 and 6 μm.

where $\gamma \approx 0.4$ and where

$$p(\zeta) = P_0 A_0 / A(\zeta)$$

and

$$w(q, \zeta) = \left(\pi \int_{\zeta q_0}^{q} \mathrm{d}q'\, q'^3 C(q') \right)^{-1/2}.$$

The function $P(q, p, \zeta)$ is given by

$$P(q, p, \zeta) = \frac{2}{\sqrt{\pi}} \int_0^{s(q,\zeta)p} \mathrm{d}x\, \mathrm{e}^{-x^2},$$

where $s(q, \zeta) = w(q, \zeta)/E^*$.

We study the contact between the solids at increasing magnification. In an apparent contact area observed at the magnification ζ, the substrate has a root-mean-square roughness amplitude [4, 10]

$$h_{\mathrm{rms}}^2(\zeta) = 2\pi \int_{\zeta q_0}^{q_1} \mathrm{d}q\, q C(q). \tag{4}$$

When we study the apparent contact area at increasing magnification, the contact pressure $p(\zeta)$ will increase and the surface roughness amplitude $h_{\mathrm{rms}}(\zeta)$ will decrease. Thus, the average separation $\bar{u}(\zeta)$, between the surfaces in the (apparent) contact regions observed at the magnification ζ, will decrease with increasing magnification.

3. Numerical results

We now present numerical results to illustrate the theory developed above. We assume a rubber block with a flat surface, squeezed by a nominal pressure P_0 against a hard solid with a randomly rough surface which we assume to be a self-affine fractal. Thus the surface roughness power spectrum for $q_0 < q < q_1$:

$$C(q) = C_0 q^{-2(1+H)}$$

where

$$C_0 = \frac{H}{\pi} \langle h^2 \rangle \left[q_0^{-2H} - q_1^{-2H} \right]^{-1} \approx \frac{H}{\pi} \langle h^2 \rangle q_0^{-2H}$$

where q_0 and q_1 are the long-distance and short-distance cut-off wavevectors, respectively.

The rubber has Young's modulus $E = 10$ MPa (as is typical for the low-frequency modulus of rubber used for seals) and Poisson ratio $\nu = 0.5$. The pressure difference in the fluid between the two sides of the seal is assumed to be $\Delta P = 0.01$ MPa, but, as long as ΔP is small compared to the pressure in the rubber–substrate nominal contact area, the leak-rate for other sealed pressures can be obtained using direct scaling (see equation (3)). If this condition is not satisfied, i.e., if $\Delta P \lesssim P_0$, it is necessary to account for the fluid pressure in solving the contact mechanics problem. This can be done in an (approximate) mean-field type approach, by assuming that the rubber–substrate contact area is determined by the squeezing pressure $P_0 - p_{\mathrm{fluid}}(\mathbf{x})$, where $p_{\mathrm{fluid}}(\mathbf{x})$ is the average local fluid pressure in the nominal rubber–substrate contact area. We assume that $L_y/L_x = 1$, but the leak-rate for other values of L_y/L_x can be obtained using direct scaling (see equation (3)). The fluid is assumed to be an incompressible Newtonian fluid with viscosity $\eta = 0.001$ N s m^{-2}. We will study how the lateral size λ_c and the height u_c of the critical constriction depend on the fractal dimension $D_f = 3 - H$ and on the root-mean-square roughness amplitude h_{rms} of the rough surface. We also present results for how the volume flow of fluid through the seals depends on D_f and h_{rms}. The randomly rough surfaces have cut-off wavevectors $q_0 = 1.0 \times 10^4$ m^{-1} and $q_1 = 7.8 \times 10^9$ m^{-1}, and we vary the applied squeezing pressure P_0 from 0.05 to 1 MPa.

Let us first vary the rms roughness amplitude. In figure 6 we show the lateral size $\lambda_c = \lambda(\zeta_c)$ and in figure 7 the height (interfacial separation) u_c of the critical constriction, as a function of the applied normal (or squeezing) pressure P_0. Results are shown for self-affine fractal surfaces with the

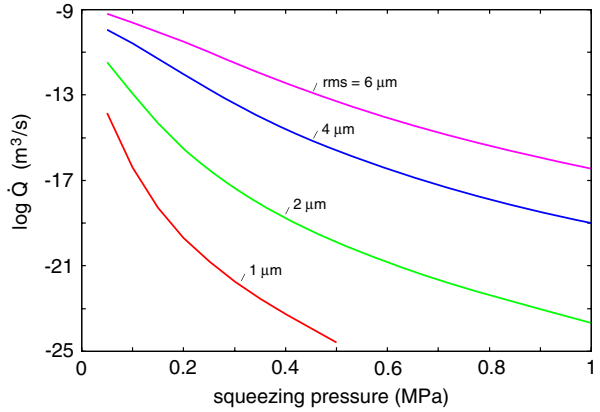

Figure 8. The volume per unit time, $\dot{Q}$, of fluid leaking through the seals as a function of the applied normal (or squeezing) pressure P_0. Results are shown for self-affine fractal surfaces with the Hurst exponent $H = 0.8$ (or fractal dimension $D_f = 2.2$), and for surfaces with the root-mean-square roughness (rms) 1, 2, 4 and 6 μm. The fluid pressure difference between the two sides is $\Delta P = 0.01$ MPa and the fluid viscosity $\mu = 10^{-3}$ N s m^{-2} (water).

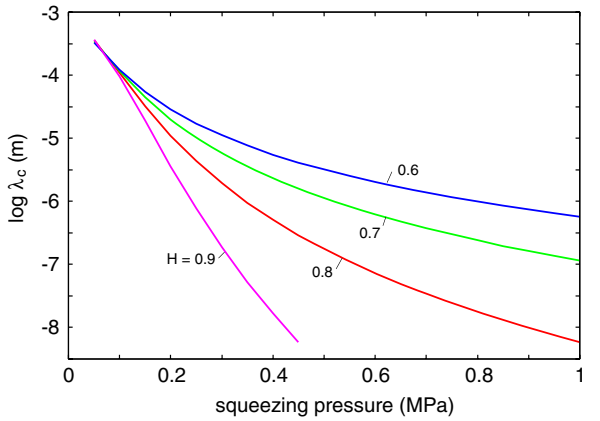

Figure 9. The lateral size $\lambda_c = \lambda(\zeta_c)$ of the critical constriction of the percolation channel, as a function of the applied normal (or squeezing) pressure P_0. Results are shown for self-affine fractal surfaces with the root-mean-square roughness (rms) 2 μm and for the Hurst exponent $H = 0.9$, 0.8, 0.7 and 0.6.

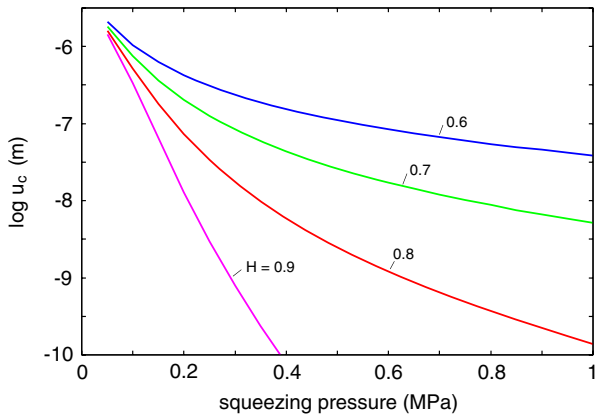

Figure 10. The interfacial separation $u_c = u_1(\zeta_c)$ at the critical constriction of the percolation channel, as a function of the applied normal (or squeezing) pressure P_0. Results are shown for self-affine fractal surfaces with the root-mean-square roughness (rms) 2 μm and for the Hurst exponents $H = 0.9$, 0.8, 0.7 and 0.6.

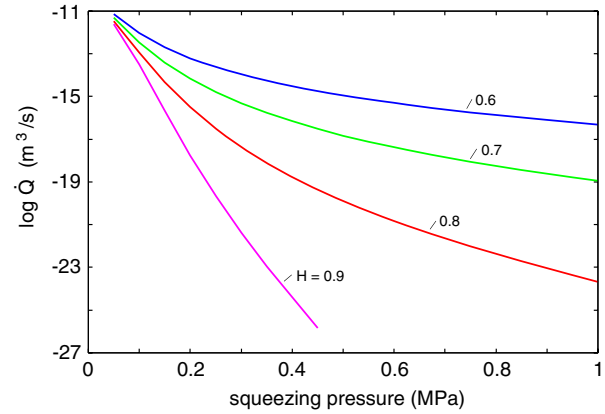

Figure 11. The volume per unit time, $\dot{Q}$, of fluid leaking through the seal as a function of the applied normal (or squeezing) pressure P_0. Results are shown for self-affine fractal surfaces with the root-mean-square roughness (rms) 2 μm and for the Hurst exponent $H = 0.9$, 0.8, 0.7 and 0.6. The fluid pressure difference between the two sides is $\Delta P = 0.01$ MPa and the fluid viscosity $\mu = 10^{-3}$ N s m^{-2} (water).

Hurst exponent $H = 0.8$ (or fractal dimension $D_f = 2.2$), and for surfaces with the root-mean-square roughness (rms) 1, 2, 4 and 6 μm. As expected, the size of the critical constriction increases when the roughness increases. In figure 8 we show the volume per unit time of fluid leaking through the seals as a function of the applied normal (or squeezing) pressure P_0. Note the extremely strong decrease in $\dot{Q}$ with increasing squeezing pressure and also its strong dependence on the rms roughness amplitude.

In figures 9–11 we show the analogous results when we vary the Hurst exponent $H = 0.9$, 0.8, 0.7 and 0.6 for $h_{rms} = 2$ μm. Note that when H decreases for a fixed h_{rms}, the short-wavelength roughness increases while the long-wavelength roughness is almost unchanged.

In figure 12 we show the interfacial separation $u_1(\zeta_c)$ and the rms roughness $h_{rms}(\zeta_c)$ in the critical constriction, as a function of the applied normal (or squeezing) pressure P_0. Results are shown for a self-affine fractal surface with the Hurst exponent $H = 0.8$ (or fractal dimension $D_f = 2.2$), and with the root-mean-square roughness (rms) 6 μm. Note that the difference between $h_{rms}(\zeta_c)$ and $u_1(\zeta_c)$ is relatively small. We have found that this is the case also for the other parameters used in the study above.

4. Molecular dynamics results

The multiscale molecular dynamics model has been described in [14], but we briefly review it here. In what follows we denote the lower solid as *substrate*, the upper solid as *block*. We are concerned with the contact between a randomly rough and rigid substrate, and an elastic block, without adhesion. We are interested in surfaces with random roughness with wavevector components in the finite range $q_1 > q > q_L$ (see figure 13), where $q_L = 2\pi/L$, L being the lateral size of the system.

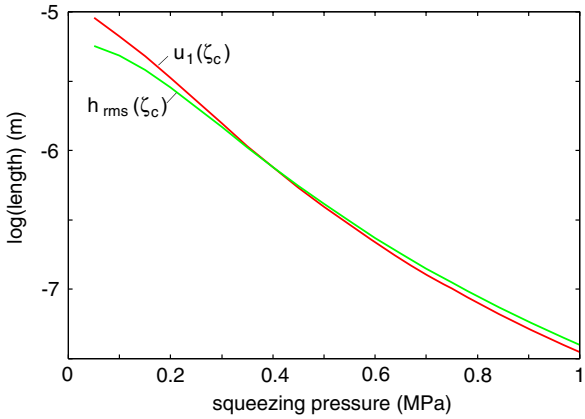

Figure 12. The interfacial separation $u_c = u_1(\zeta_c)$ and the rms roughness $h_{rms}(\zeta_c)$ in the critical constriction of the percolation channel, as a function of the applied normal (or squeezing) pressure P_0. Results are shown for self-affine fractal surfaces with the Hurst exponent $H = 0.8$ (or fractal dimension $D_f = 2.2$), and with the root-mean-square roughness (rms) 6 μm.

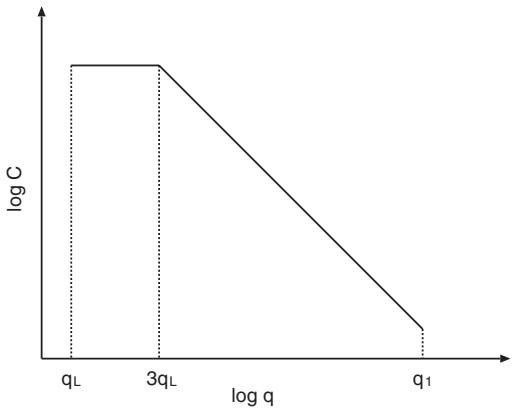

Figure 13. Surface roughness power spectrum of a surface which is self-affine fractal for $q_1 > q > 3q_L$. The slope log C–log q relation for $q > 3q_L$ determines the fractal exponent of the surface. The lateral size L of the surface determines the smallest wavevector $q_L = 2\pi/L$.

In order to accurately study contact mechanics between elastic solids, it is necessary to consider a solid block which extends a distance $\sim L$ in the direction normal to the nominal contact area. This requires a huge number of atoms or dynamical variables even for small systems. Therefore we developed a multiscale molecular dynamics approach to study contact mechanics to avoid this trouble [14]. The lateral size of the system is $L = 1040$ Å. $L_x = N_x a$ and $L_y = N_y a$, where $a = 2.6$ Å is the lattice space of the block, $N_x = N_y = 400$ for the block[1]. The elastic modulus and Poisson ratio are $E = 77.2$ GPa and $\nu = 0.42$. The lattice space of the substrate is $b \approx a/\phi$, where $\phi = (1+\sqrt{5})/2$ is the golden mean, in order to achieve (nearly) incommensurate structures at the interface.

For self-affine fractal surfaces, the power spectrum has a power-law behavior $C(q) \sim q^{-2(H+1)}$, where the Hurst exponent H is related to the fractal dimension D_f of the surface via $H = 3 - D_f$. For real surfaces this relation holds only for a finite wavevector region $q_1 < q < q_0$, where $q_1 = 2\pi/b$, q_0 is the roll-off wavevector $q_0 = 3q_L$ (see figure 13). The randomly rough surfaces have been generated as described in [3, 14] and have root-mean-square roughness $h_{rms} = 10$ Å and fractal dimension $D_f = 2.2$. The roll-off wavevector $q_0 = 3q_L$, where $q_L = 2\pi/L$ and $L = 1040$ Å. In this section we define the magnification $\zeta = q/q_L$.

The atoms at the interface between block and substrate interact with repulsive potential $U(r) = \epsilon(r_0/r)^{12}$, where r is the distance between a pair of atoms, $r_0 = 3.28$ Å and $\epsilon = 74.4$ meV. In molecular dynamics simulations there is no unique definition of contact (see [14]). Here we use the critical distance d_c to define contact. If the separation between two atoms is smaller than d_c it has been denoted as contact, otherwise non-contact. Here $d_c = 4.36$ Å.

Figure 14 shows the block–substrate contact regions at different magnifications $\zeta = 1, 3, 6, 9, 12, 648$. Note that when the magnification is increased from 9 to 12, the non-contact region percolates. The percolation occurs when the normalized projected contact area $A/A_0 \approx 0.4$, in good agreement with percolation theory [13].

5. Improved analytical description

In section 2 we assumed that all the fluid flow occurs through a single constriction, which we refer to as the critical constriction. In reality, fluid flow will also occur in other flow channels even if they have more narrow constrictions. In this section we will assume that there is a finite concentration of critical or nearly critical constrictions, which correspond to all constrictions appearing when the magnification changes in some narrow interval around the critical value ζ_c, e.g., in such a way that $A(\zeta)/A_0$ changes by, say, ± 0.03. Since we are very close to the percolation threshold, we will assume that the size of all the (nearly critical) constrictions remains the same. In a more accurate treatment one would instead introduce a distribution of sizes of constrictions. In figure 15(a) the dots correspond to the critical or nearly critical constrictions along percolation channels (solid lines). One expects the (nearly critical) constrictions to be nearly randomly distributed in the apparent contact area, and that the channels, of which they are part, have all possible directions as indicated by the lines in figure 15(a). Here we will consider a simplified version of (a) where the (nearly critical) constrictions form a more ordered arrangement as in figure 15(b). In reality, the dots and the lines should be (nearly) randomly distributed as in15(a), but this is likely to have only minor effects on what follows.

[1] The length scale in the MD simulations is, of course, very different from that involved in most applications to seals. However, there is no natural length scale in the elastic continuum description, and in numerical studies it is the grid-size which introduces the relevant (shortest) length scale. Thus the 'lattice constant' in our MD simulations can also be interpreted as the grid-size in an elastic continuum representation of our seal problem. If the grid-size is smaller than the wavelength of any of the (relevant) surface roughness components, then the result of our simulation can be reinterpreted as giving the contact mechanics for macroscopic solids. Thus, our results are very general and valid also for macroscopic systems. We also note that the contact mechanics only depends on the ratio P_0/E between the squeezing pressure and the elastic modulus, and our MD simulation results are therefore unchanged if we simultaneously reduce P_0 and E to values typically in rubber applications (e.g., $E \approx 10$ MPa and $P_0 = 0.5$ MPa).

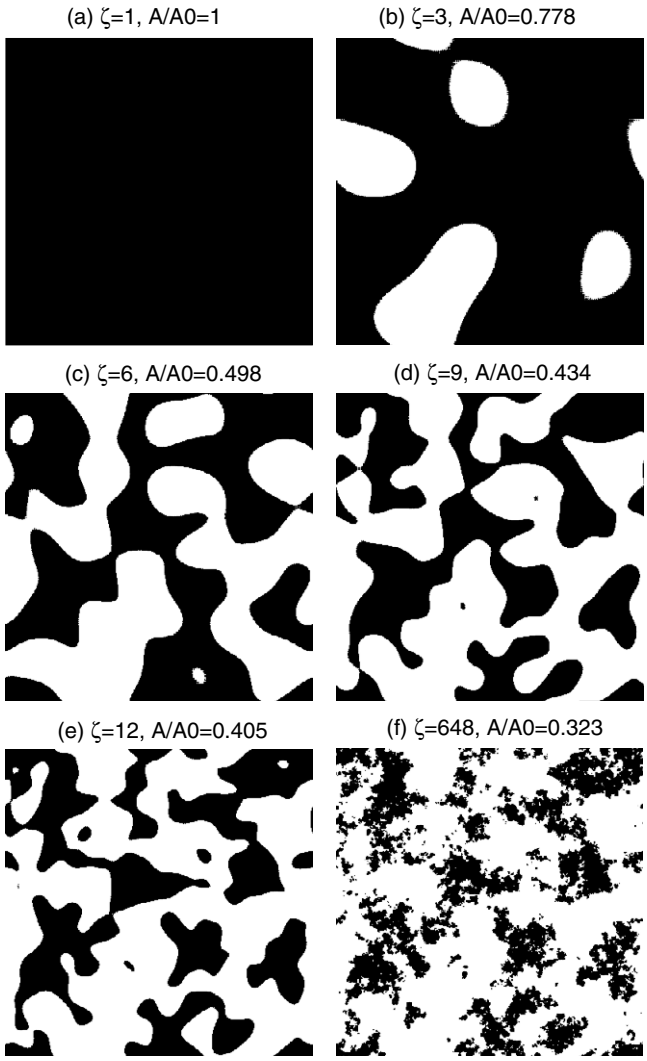

Figure 14. The contact regions at different magnifications $\zeta = 1, 3, 6, 9, 12, 648$, are shown in (a)–(f) respectively. The pressure is $p \approx 4.1$ GPa. When the magnification is increased from 9 to 12, the non-contact region percolates.

On average the fluid will only flow in the x-direction. Thus, in a first approximation one may assume that no fluid flows along the (transverse) channels pointing (mainly) in the y-direction in figure 15(b). Let a be the (average) distance between two nearby critical constrictions. Thus we expect $n = L_x/a$ constrictions along a percolation channel (in the figure we have $n = 3$). If $\dot{Q}_1$ denotes the fluid volume per unit time flowing along one percolation channel, then we must have

$$\dot{Q}_1 = M(P_a - P_1) = M(P_1 - P_2) = \cdots = M(P_n - P_b). \quad (5)$$

From (5) we get

$$\dot{Q}_1 = \frac{M}{n}(P_a - P_b).$$

As expected, the amount of fluid flowing in the channel is reduced when the number of constrictions increases. However, there will be roughly L_y/a percolation channels so the total

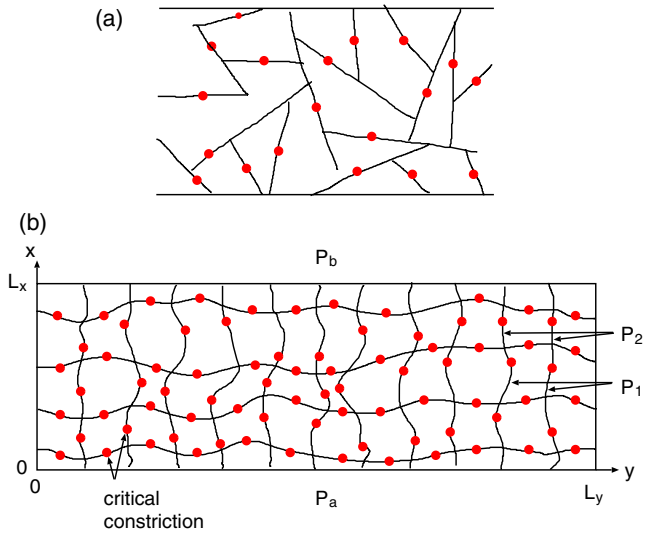

Figure 15. The solid lines denote non-contact channels and the dots critical, or near critical, constrictions. In reality the constrictions and channels are nearly randomly distributed as in (a) (see also figure 14(e)) but in the model calculation we use the more ordered structure shown in (b).

fluid flow will be

$$\dot{Q} = \frac{L_y}{L_x} M(P_a - P_b) \quad (6)$$

which is identical to the result obtained in section 2. This analysis is very rough, and a more detailed analysis will result in some modifications of the leak-rate, but (6) should be very useful as a first rough estimate of the leak-rate. Note that the present treatment will result in a more gradual change in the liquid pressure in the apparent contact region, from the initial high pressure value P_a (entrance side) to the low pressure value P_b (exit side).

6. Comparison with experiment

We have not found any results in the literature concerning leak-rates of seals for well-characterized systems. However, we have found some results which are in qualitative agreement with our theory. For example, leak-rates observed for both rubber and steel seals tend to decrease very fast (roughly exponentially) with increasing contact force. Thus, in [15] the leak-rate for a rubber seal decreased by 6 orders of magnitude as the load increased by a factor of 10. A similar sharp drop in the leak-rate with increasing contact force has been observed for seals made from steel [16]. However, in the latter case some plastic deformation is likely to occur in the contact region. In both cases the nominal pressure may change less than the change in the load, due to an increase in the nominal contact area with increasing load. A detailed analysis of the experimental data is not possible as the surface topography was not studied in detail. In section 9 we suggest a simple experiment which can be used to test the theory.

The present theory implies that most of the fluid leakage occurs through the critical or nearly critical constrictions in

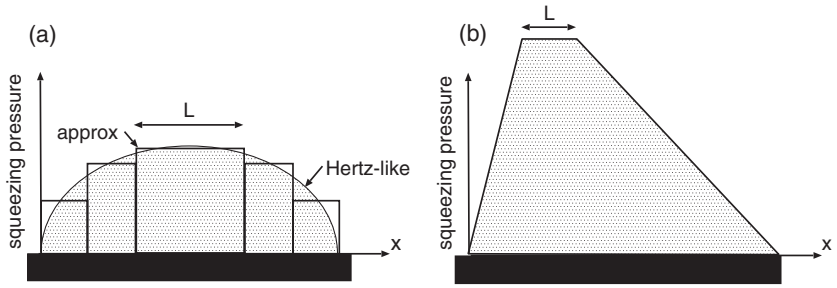

Figure 16. Nominal contact pressure distribution $P_0(x)$ (curve bounding the dotted area) for (a) O-ring seal and (b) lip-seal. In (a) the curve denoted by 'approx' is an approximation to the continuous Hertz-like curve.

the percolating channels at the interface between the two solids. Since the constrictions are very small they can easily be clogged up by dirt particles in the fluid. This results in leak-rates which decrease with increasing time as the microscopic gaps get clogged up. This has recently been observed for metal seals [16]. In fact, by using specially prepared fluids with immersed particles having a narrow distribution of particle diameters, it should be possible to determine (approximately) the size (or rather the height) of the critical constriction.

7. Comment on the role of non-uniform pressure, rubber viscoelasticity and adhesion

In the study above we have assumed that the normal (squeezing) pressure is constant in the nominal rubber–countersurface contact region. In reality, this is (almost) never the case. Thus, in rubber O-ring applications one expects a pressure distribution which is Hertzian-like, as indicated in figure 16(a). In (dynamical) rubber seals for linear reciprocal motion, the pressure distribution is asymmetric, with a much steeper increase in the pressure when going from the high pressure (P_a) fluid side towards the center of the seal, as compared to going from the low pressure (P_b) fluid side toward the center of the seal, see figure 16(b). (The reason for this asymmetry does not interest us here.) The theory developed above can be applied approximately to these cases too. Thus in case (a) (e.g., rubber O-ring seals) one may approximate the actual Hertzian-like pressure profile with a sum of step functions as indicated in figure 16(a). Since the seal-action is so strongly dependent on the squeezing pressure (see figures 8 and 11), it is enough to include the central step region (with width L) in the analysis. Since there is no unique way to determine the width L there will be some (small) uncertainty in the analysis, but this is not important in most practical cases. Similarly, for the lip-seal (figure 16(b)) during the stationary condition it is enough to include the region (width L) where the normal pressure is maximal.

In the study above we have assumed that the rubber behaves as a purely elastic solid. In reality, rubber-materials are viscoelastic. One consequence of this is stress relaxation. For example, after a rubber O-ring has been deformed to fit into the 'cavity' where it is placed, the stress exerted on the solid walls will decrease with increasing time. Since rubber-materials have very wide distribution of relaxation times, the stress can continue to decrease even one year after installation. Thus, after very long time the pressure in the rubber–countersurface contact region may be so low that the seal fails (note: we found earlier that the leak-rate depends extremely sensitively on the normal pressure). Stress relaxation can be easily taken into account approximately in the analysis above by using an effective relaxation modulus $E_{\rm eff}(t)$ (where t is time)[2], obtained from the frequency dependent viscoelastic modulus $E(\omega)$, which can be measured using standard methods.

Now let us comment on the role of adhesion in rubber seals. We first note that if the fluid is an oil, the effective adhesion between the rubber and the hard countersurface may vanish, or nearly vanish, as observed in some experiments [17]. If the fluid is not an oil (e.g., water) some effective adhesive interaction may remain. In particular, if the fluid is a gas then the effective adhesion may be similar to that in the normal atmosphere. However, even in this case the adhesive interaction between the solids may have a negligible influence on the leak-rate. The reason for this is that adhesion operates mainly at very short length scales, corresponding to high magnification $\zeta > \zeta_{\rm ad}$, while the leak-rate is determined mainly by the contact mechanics at the point where the first percolation channel appears, corresponding to the magnification ζ_c. If $\zeta_c \ll \zeta_{\rm ad}$ the adhesive interaction will have a negligible influence on the leak-rate. We now illustrate this with a numerical calculation using the theory of [7].

Figure 17 shows the relative contact area $A(\zeta)/A_0$ as a function of the logarithm of the magnification ζ. Note that at the magnification ζ_c, where the non-contact area first percolates, the adhesional interaction has no influence on the contact area. The adhesional interaction will manifest itself only for $\zeta > \zeta_{\rm ad}$, where the adhesional interaction increases the contact area as compared to the case without the adhesional interaction included. The result in figure 17 is for a rubber block in contact with a hard solid with a self-affine fractal surface with the root-mean-square roughness $h_{\rm rms} = 6\ \mu$m,

[2] The simplest approximation is to replace E with the relaxation modulus $E(t)$, but this is a very crude approximation even though it has been used in the literature (e.g., in [21]). In [10] one of the present authors has studied this problem in detail, and shown how the contact mechanics can be correctly described for viscoelastic solids by replacing E with $E_{\rm eff}(t)$ defined by

$$\frac{1}{E_{\rm eff}(t)} = \frac{1}{2\pi}\int_{-\infty}^{\infty} {\rm d}\omega \frac{1-\exp({\rm i}\omega T)}{-{\rm i}\omega}\frac{\exp(-{\rm i}\omega t)}{E(\omega)},$$

where $E(\omega)$ is the frequency dependent viscoelastic modulus and T an arbitrary time with $t < T$.

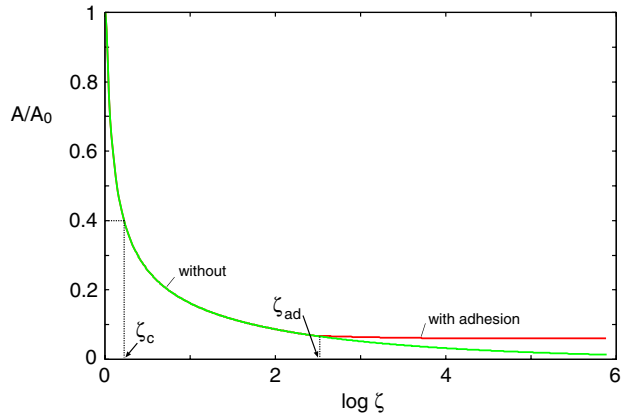

Figure 17. The relative contact area $A(\zeta)/A_0$ as a function of the logarithm of the magnification ζ. Note that at the magnification ζ_c, where the non-contact area first percolates, the adhesional interaction has no influence on the contact area. The adhesional interaction will manifest itself only for $\zeta > \zeta_{ad}$, where the adhesional interaction increases the contact area as compared to the case without the adhesional interaction included. For a rubber block in contact with a hard solid with a self-affine fractal surface with the root-mean-square roughness $h_{rms} = 6\ \mu$m, the Hurst exponent $H = 0.8$. The squeezing pressure $P_0 = 0.2$ MPa and, for the curve 'with adhesion', with the interfacial binding energy per unit area $\Delta\gamma = 0.05$ J m^{-2}.

the Hurst exponent $H = 0.8$, and for the squeezing pressure $P_0 = 0.2$ MPa.

Finally we note that if there is very little fluid at the interface strong capillary adhesion may occur between the surfaces. This is known to be of great importance in, e.g., the context of rubber wiper blades. This topic has been discussed in detail in [18, 19].

8. Dynamical seals

The theory presented above is for static seals. Here we give some comments related to dynamical seals. We will estimate the leak-rate for linear reciprocal seals at very low sliding velocity. We assume that the roughness occurs mainly on the rubber surface and we treat the hard countersurface as perfectly flat. Thus, as the rubber slides along the countersurface the contact mechanics does not change, e.g., the percolation channel will be time independent in the reference frame moving with the rubber. We consider the system in the reference frame where the rubber is stationary while the hard countersurface moves from left to right with the velocity v_0. The rubber is assumed to be below the countersurface, see figure 18. The high pressure fluid region (pressure P_a) occupies $x < 0$ while the low pressure region (pressure P_b) occupies $x > L$.

We assume a Newtonian fluid and stationary and laminar flow. The basic equations for the fluid flow are

$$\nabla p = \eta \nabla^2 \mathbf{v}, \qquad \nabla \cdot \mathbf{v} = 0,$$

where $p(\mathbf{x})$ and $\mathbf{v}(\mathbf{x})$ are the fluid pressure and the fluid flow velocity, respectively. We now consider the fluid flows in the percolation channel. Let s be the length-coordinate along

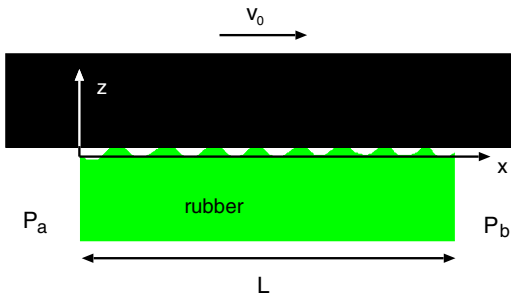

Figure 18. A rubber block with a rough surface in contact with a hard smooth countersurface (upper block) which moves relative to the rubber block with the velocity v_0.

the percolation channel. Since in general the $\lambda(s) \gg u(s)$, where $\lambda(s)$ is the width and $u(s)$ the height of the channel at the point s along the channel, we can write the velocity as $\mathbf{v}(\mathbf{x}) = \hat{s}v(s, z)$ where

$$v(s, z) \approx \frac{1}{2\eta}\frac{dp}{ds} z(z - u(s)) + v_0 \hat{x} \cdot \hat{s} \frac{z}{u(s)}.$$

The volume flow per unit time through any cross-section of the channel is assumed to be the same, and equal to $\dot{Q}$ which gives

$$\dot{Q} = \lambda(s) \int_0^{u(s)} dz\ v(s)$$
$$= \lambda(s) \left(-\frac{u^3(s)}{12\eta}\frac{dp}{ds} + v_0 \hat{x} \cdot \hat{s} \frac{u(s)}{2} \right)$$

or

$$\frac{dp}{ds} = \frac{6\eta}{u^2(s)} v_0 \hat{x} \cdot \hat{s} - \frac{12\eta \dot{Q}}{\lambda(s) u^3(s)}.$$

Integrating this equation gives

$$p(l_a) = P_a + \int_0^{l_a} ds \left[\frac{6\eta}{u^2(s)} v_0 \hat{x} \cdot \hat{s} - \frac{12\eta \dot{Q}}{\lambda(s) u^3(s)} \right] \qquad (7)$$

where l_a is the length of the percolation channel. Let $\tilde{P}(u)$ be the probability to find the surfaces separated by a height u along the percolation channel. Note that $\lambda(s)$ can also (at least locally) be considered as a function of u, which we denote by $\lambda(u)$ for simplicity. Thus we can write (7) as

$$p(l_a) = P_a + 6L_a \eta v_0 \int_{u_c}^{\infty} du\ \frac{\tilde{P}(u)}{u^2} - 12 l_a \eta \dot{Q} \int_{u_c}^{\infty} du\ \frac{\tilde{P}(u)}{\lambda(u) u^3} \qquad (8)$$

where L_a is the length of the percolation path projected on the x-axis. In [9] we have shown how it is possible to calculate the distribution $\bar{P}_u$ of heights u between two surfaces in elastic contact. We will now assume that (note: $u > u_c$)

$$\tilde{P}(u) \approx \frac{\bar{P}_u}{\int_{u_c}^{\infty} du'\ \bar{P}_{u'}}.$$

Let us write (8) as

$$p(l_a) = P'_a = P_a + B_a v_0 - C_a \dot{Q} \qquad (9)$$

where

$$B_a = 6L_a\eta \int_{u_c}^{\infty} du\ \frac{\tilde{P}(u)}{u^2} \tag{10}$$

and

$$C_a = 12l_a\eta \int_{u_c}^{\infty} du\ \frac{\tilde{P}(u)}{\lambda(u)u^3}. \tag{11}$$

Similarly, one gets[3]

$$p(l_b) = P_b' = P_b - B_b v_0 - C_b \dot{Q}. \tag{12}$$

Thus in this case (1) takes the form

$$\dot{Q} = M(P_a' - P_b')$$
$$= M(P_a - P_b) + M(B_a + B_b)v_0 - M(C_a - C_b)\dot{Q}$$

or

$$\dot{Q} = M\frac{\Delta P + (B_a + B_b)v_0}{1 - M(C_a - C_b)}. \tag{13}$$

The factor $M(C_a - C_b)$ in the denominator in this expression is independent of v_0 and we will assume that it is negligible compared to unity and neglect it. One interesting application of (13) is to wiper blades. Here $\Delta P = 0$ so that (13) takes the form

$$\dot{Q} = M(B_a + B_b)v_0. \tag{14}$$

Substituting (2) and (10) (and a similar expression for B_b) in (14) gives

$$\dot{Q} = L_y u_c^3 v_0 \frac{\alpha}{2} \int_{u_c}^{\infty} du\ \frac{\tilde{P}(u)}{u^2} \tag{15}$$

where we have included the extra factor L_y/L_x to take into account the number of square seal units. During the time t the leak-volume is $\dot{Q}t$. We define the average thickness d of the leak-film as $d = \dot{Q}t/(L_y v_0 t)$. From (15) we get

$$d = \beta u_c \tag{16}$$

$$\beta = \frac{\alpha}{2} \int_{u_c}^{\infty} du\ u_c^2 \frac{\tilde{P}(u)}{u^2}. \tag{17}$$

We have calculated the integral I in β for some typical cases[4], and found that $I \approx 0.1$–0.2 so we expect $\beta \approx 0.1$.

In the treatment above we have assumed that the contact between the rubber and the hard countersurface does not depend on the pressure in the fluid, which is a good approximation as long as the fluid pressure $p(\mathbf{x}) \ll P_0$. However, as the sliding velocity increases, the fluid pressure in some regions at the interface will increase, which will tend to increase the separation between the two surfaces. At very high sliding velocity, hydrodynamic lubrication will prevail and the surfaces are completely separated by a thin fluid film. However, even at much lower sliding velocity the hydrodynamic pressure buildup may strongly increase the leak-rate. In particular, the pressure at the critical constriction will tend to increase the separation between the surfaces and hence increase the leak-rate. We will not study this effect here but just estimate when this effect becomes important. Let p_c be the pressure at the critical constriction. If p_c acts over the area λ_c^2 it will locally increase the separation between the surfaces by an amount[5] $\Delta u \approx \lambda_c p_c/E$. Thus, the pressure at the critical constriction must be much smaller than Eu_c/λ_c in order for the pressure induced effect to be negligible. Note that

$$p_c \approx 6L\eta v_0 \int_{u_c}^{\infty} du\ \frac{\tilde{P}(u)}{u^2} \tag{18}$$

so the present study is limited to sliding velocities

$$v_0 \ll \frac{Eu_c^3}{6L\eta\lambda_c}\left(\int_{u_c}^{\infty} du\ u_c^2\frac{\tilde{P}(u)}{u^2}\right)^{-1} \approx \frac{Eu_c^3}{L\eta\lambda_c} \tag{19}$$

where we have used that the integral typically is of order $\sim$0.15. Thus, for example, in a wiper blade application [20], after some use the rubber blades typically develop (because of wear) a surface roughness with an rms amplitude of several micrometer. If the rms roughness is 2 μm (and the Hurst exponent $H = 0.8$), the nominal pressure $\sim$0.2 MPa, and if we assume that $E \approx 10$ MPa we get from figures 7 and 6 $u_c \approx 0.1$ μm and $\lambda_c \approx 10$ μm. If $L \approx 0.1$ mm and (for water) $\eta \approx 10^{-3}$ Pa s we get that the slip velocity must be at most $\sim$1 cm s^{-1} in order for (17) to be valid. According to (16) the (average) film thickness of the water layer would be of order 0.01 μm.

9. A new experiment

Very few studies of leak-rates of seals with well-characterized surfaces have been published. Here we would like to suggest a very simple experiment which could be used to test the theory presented in section 2. In figure 19 we show a set-up for measuring the leak-rate of seals. A glass (or PMMA) cylinder with a rubber ring (with rectangular cross-section) glued to one end is squeezed against a hard substrate with well-defined surface roughness. The cylinder is filled with a fluid, e.g., water, and the leak-rate of the fluid at the rubber–countersurface is detected by the change in the height of the

[3] We assume that no cavitation occurs at the exit of the critical constriction. Cavitation may occur if the local pressure at the exit of the critical constriction is negative, but in this paper we assume a sufficiently low sliding velocity v_0 that this is not the case. If cavitation occurs $p(l_b) \approx 0$, or, more accurately, $p(l_b)$ is equal or close to the vapor pressure of the fluid or of gases dissolved in the fluid. We note that the transition from boundary (or mixed lubrication) to hydrodynamic lubrication probably involves cavitation at the exit of many narrow constrictions, since otherwise the total load supported by the fluid film would be very small. It would be very interesting to study this problem theoretically, since the transition from boundary lubrication to hydrodynamic lubrication is not well understood.

[4] We did two calculations: for a self-affine fractal surface with the rms roughness of $h_{rms} = 2$ μm and the squeezing pressure $P_0 = 0.18$ MPa we got $B \approx 0.11$ (and $u_c \approx 0.1$ μm and $\lambda_c \approx 16$ μm) and for $h_{rms} = 4$ μm and $P_0 = 0.2$ MPa we got $B \approx 0.21$ (and $u_c \approx 1$ μm and $\lambda_c \approx 109$ μm).

[5] The fluid pressure along the percolation channel increases towards the critical constriction. Thus, the elastic deformation of the rubber at the critical constriction is determined not just by the pressure at the constriction but also by the pressure acting on the rubber along the percolation path. If one assumes a straight percolation path and that the pressure along the percolation path $p(x) = p_c x/L$ then one can easily show that $\Delta u \approx \ln(L/\lambda_c)\lambda_c p_c/E$ but the additionally logarithmic factor is never very large and does not change our qualitative conclusion.

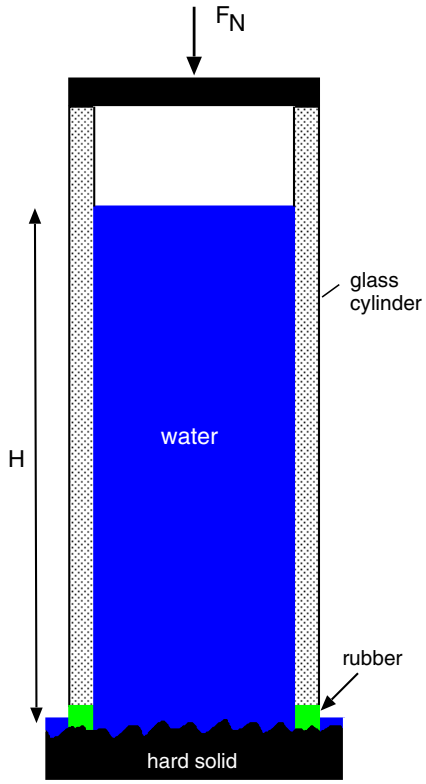

Figure 19. A simple experimental set-up for measuring the leak-rate of seals. A glass (or PMMA) cylinder with a rubber ring glued to one end is squeezed against a hard substrate with well-defined surface roughness. The cylinder is filled with a fluid, e.g., water, and the leak-rate of the fluid at the rubber–countersurface is detected by the change in the height of the fluid in the cylinder. In this case the pressure difference $\Delta P = P_a - P_b = \rho g H$, where g is the gravitation constant, ρ the fluid density and H the height of the fluid column. With $H \approx 1$ m we get typically $\Delta P \approx 0.01$ MPa.

fluid in the cylinder. In this case the pressure difference $\Delta P = P_a - P_b = \rho g H$, where g is the gravitation constant, ρ the fluid density and H the height of the fluid column. With $H \approx 1$ m we get typically $\Delta P \approx 0.01$ MPa. With the diameter of the glass cylinder of order a few cm, the condition $P_0 \gg \Delta P$ (which is necessary in order to be able to neglect the influence on the contact mechanics from the fluid pressure at the rubber–countersurface) is satisfied already for loads (at the upper surface of the cylinder) of the order of kg.

10. Summary and conclusion

Seals are extremely useful devices to prevent fluid leakage. However, the exact mechanism of roughness induced leakage is not well understood. We have presented a theory of the leak-rate of seals, which is based on percolation theory and a recently developed contact mechanics theory. We have studied both static and dynamic seals. We have presented numerical results for the leak-rate $\dot{Q}$, and for the lateral size λ_c and the height u_c of the critical constriction. We assumed self-affine fractal surfaces and presented results for how $\dot{Q}$, λ_c and u_c depend on the root-mean-square roughness amplitude and the fractal dimension $D_f = 3-H$ (where H is the Hurst exponent), and on the pressure P_0 with which the rubber is squeezed against the rough countersurface.

We have also presented molecular dynamics results which show that when two elastic solids with randomly rough surfaces are squeezed together, as a function of increasing magnification or decreasing squeezing pressure, a non-contact channel will percolate when the relative projected contact area, A/A_0, is of the order of 0.4, in accordance with percolation theory. Finally, we have suggested a simple experiment which can be used to test the theory.

The theory we have presented in this paper is very rough, but we believe that it captures the most important physics, and that the approach presented can be improved and extended in various ways.

Acknowledgments

We thank Ed Widder (Federal Mogul Sealing Systems) and Matthias Schmidt (IFAS, RWTH Aachen University) for useful correspondence related to seals. We also thank A Koenen (Valeo Systeme d'Essuyage) for very interesting information related to the tribological properties of the contact between rubber and glass in the context of rubber wiper blades.

References

[1] Flitney R 2007 *Seals and Sealing Handbook* (Amsterdam: Elsevier)
[2] Mofidi M, Prakash B, Persson B N J and Albohr O 2008 *J. Phys.: Condens. Matter* **20** 085223
[3] See, e.g., Persson B N J, Albohr O, Tartaglino U, Volokitin A I and Tosatti E 2005 *J. Phys.: Condens. Matter* **17** R1
[4] Persson B N J 2001 *J. Chem. Phys.* **115** 3840
[5] Persson B N J 2007 *Phys. Rev. Lett.* **99** 125502
[6] Persson B N J 2006 *Surf. Sci. Rep.* **61** 201
[7] Persson B N J 2002 *Eur. Phys. J.* E **8** 385
[8] Persson B N J, Bucher F and Chiaia B 2002 *Phys. Rev.* B **65** 184106
[9] Yang C and Persson B N J 2008 *J. Phys.: Condens. Matter* **20** 215214
[10] Persson B N J, Albohr O, Creton C and Peveri V 2004 *J. Chem. Phys.* **120** 8779
[11] Greenwood J A and Williamson J B P 1966 *Proc. R. Soc.* A **295** 300
[12] Bush A W, Gibson R D and Thomas T R 1975 *Wear* **35** 87
[13] Stauffer D and Aharony A 1991 *An Introduction to Percolation Theory* (Boca Raton, FL: CRC Press)
[14] Yang C, Tartaglino U and Persson B N J 2006 *Eur. Phys. J.* E **19** 47
[15] Widder E 2004 *ASME B46 Seminar (April 15)*
[16] Schmidt M, Murrenhoff H, Lohrberg H and Körber F-J 2008 at press
[17] Zappone B, Rosenberg K J and Israelachvili J 2007 *Tribol. Lett.* **26** 191
[18] Persson B N J 2008 *J. Phys.: Condens. Matter* **20** 315007
[19] Deleau F, Mazuyer D and Koenen A 2008 *Tribol. Int.* at press
[20] Koenen A and Sanon A 2007 *Tribol. Int.* **40** 1484
[21] Creton C and Leibler L 1996 *J. Polym. Sci.* B **34** 190